# Inhibition of Poly(ADP-Ribose) Polymerase Enhances Cell Death and Improves Tumor Growth Delay in Irradiated Lung Cancer Models

Jeffrey M. Albert,[1] Carolyn Cao,[1] Kwang Woon Kim,[1] Christopher D. Willey,[1] Ling Geng,[1] Dakai Xiao,[1] Hong Wang,[1] Alan Sandler,[1] David H. Johnson,[1] Alexander D. Colevas,[2] Jennifer Low,[2] Mace L. Rothenberg,[1] and Bo Lu[1]

**Abstract**

**Purpose:** Poly(ADP-ribose) polymerase-1 (PARP-1) is the founding member of a family of enzymes that catalyze the addition of ADP-ribose units to proteins that mediate DNA repair pathways. Ionizing radiation induces DNA strand breaks, suggesting that PARP-1 inhibition may sensitize tumor cells to radiation.

**Experimental Design:** We investigated the combination of PARP-1 inhibition with radiation in lung cancer models. ABT-888, a novel potent PARP-1 inhibitor, was used to explore the effects of PARP-1 inhibition on irradiated tumors and tumor vasculature.

**Results:** ABT-888 reduced clonogenic survival in H460 lung cancer cells, and inhibited DNA repair as shown by enhanced expression of DNA strand break marker histone γ-H2AX. Both apoptosis and autophagy contributed to the mechanism of increased cell death. Additionally, ABT-888 increased tumor growth delay at well-tolerated doses in murine models. For a 5-fold increase in tumor volume, tumor growth delay was 1 day for ABT-888 alone, 7 days for radiation alone, and 13.5 days for combination treatment. Immunohistochemical staining of tumor sections revealed an increase in terminal deoxyribonucleotide transferase–mediated nick-end labeling apoptotic staining, and a decrease in Ki-67 proliferative staining after combination treatment. Matrigel assay showed a decrease in *in vitro* endothelial tubule formation with ABT-888/radiation combination treatment, and von Willebrand factor staining of tumor sections revealed decreased vessel formation *in vivo*, suggesting that this strategy may also target tumor angiogenesis.

**Conclusions:** We conclude that PARP-1 inhibition shows promise as an effective means of enhancing tumor sensitivity to radiation, and future clinical studies are needed to determine the potential of ABT-888 as a radiation enhancer.

Poly(ADP-ribose) polymerase-1 (PARP-1) is a highly conserved zinc finger DNA-binding protein that uses $NAD^+$ as a substrate to attach ADP-ribose units to glutamate residues of proteins that are involved in DNA repair. These proteins include histones, topoisomerases, helicases, single-strand break repair, and base-excision repair proteins. PARP has been implicated in the $G_2$-M cell cycle checkpoint (1), and the use of PARP-/- knockout mice has shown that PARP plays an important role in DNA damage recovery (2). Specifically, PARP has been shown to be an important mediator of DNA base excision repair (3, 4), which is important in the repair of single-stranded breaks. Moreover, PARP is also known to bind the more lethal double-stranded DNA breaks (5). Interestingly, the catalytic activity of PARP-1 is stimulated >500-fold upon binding DNA breaks (6).

Ionizing radiation induces DNA strand breaks, which mediate its cytotoxic effects. The various types of DNA damage induced by radiation result in activation of proteins that mediate repair pathways, such as PARP, DNA-activated protein kinase, p53, and the protein product of the ataxia-telangiectasia mutated (*ATM*) gene (7). Therefore, inhibiting DNA repair in tumor cells is a rational therapeutic strategy to enhance the effects of radiation. PARP-1 has been specifically shown to bind DNA strand breaks formed by ionizing radiation to facilitate repair (8), implicating it as an attractive target for radiation enhancement. Indeed, inhibiting PARP-1 activity has been established as an effective means of sensitizing cells to DNA-damaging agents (9). AG14361, a small-molecule PARP-1 inhibitor, has also recently shown promise in preclinical models (10, 11). Moreover, one study found that PARP inhibitors

**Authors' Affiliations:** [1]Vanderbilt Ingram Cancer Center, Vanderbilt University School of Medicine, Nashville, Tennessee and [2]National Cancer Institute, Bethesda, Maryland

Received 12/4/06; revised 2/16/07; accepted 3/5/07.

**Grant support:** 5 U01 CA099177-04, Vanderbilt Physician Scientist Grant, a grant from the Mesothelioma applied research foundation, and Department of Defense grants PC031161 and BC030542.

The costs of publication of this article were defrayed in part by the payment of page charges. This article must therefore be hereby marked *advertisement* in accordance with 18 U.S.C. Section 1734 solely to indicate this fact.

**Requests for reprints:** Bo Lu, Department of Radiation Oncology, Vanderbilt University, 1301 22nd Avenue South, B-902 The Vanderbilt Clinic, Nashville, TN 37232-5671. Phone: 615-343-9233; Fax: 615-343-3075; E-mail: bo.lu@vanderbilt.edu.



doi:10.1158/1078-0432.CCR-06-2872

sensitize tumor cells to low-dose ionizing radiation *in vitro*, further supporting the clinical viability of this strategy (12).

Lung cancer is the second most common cause of cancer in both men and women in the United States, and the leading cause of cancer deaths. Lung cancer has a dismal prognosis with 5-year relative survival rates of only 13.6% for men and 17.5% for women, so improved therapies are needed (13). Additionally, it has been shown through both preclinical models and retrospective clinical analysis that enhanced DNA repair capacity is associated with chemotherapy resistance and poor survival in non–small cell lung cancer patients (14, 15). Also, enhanced DNA repair has been suggested to be involved in lung cancer radioresistance (16, 17). We therefore chose to investigate the combination of the novel PARP-1 inhibitor, ABT-888, and radiotherapy in H460 human non–small cell lung cancer models.

## Materials and Methods

***Cell culture and drug treatment.*** H460 lung carcinoma cells were obtained from American Type Culture Collection and maintained in RPMI 1640 with 10% fetal bovine serum and 1% penicillin/streptomycin. Human umbilical vein endothelial cells were obtained from Clonetics and maintained in EBM-2 medium supplemented with EGM-2 MV single aliquots (BioWhittaker). ABT-888 (Abbott Laboratories) was dissolved in DMSO and kept as 10 mol/L stock solutions in small aliquots at -20°C. Radiation was given by use of a $^{137}$Cs irradiator (J.L. Shepherd and Associates).

***Immunofluorescence for γ-H2AX DNA repair marker.*** H460 cells were grown on sterile histologic slides with 15 mL medium. After 24 h, the cells were incubated with ABT-888 5 μmol/L and then immediately irradiated with either 0 or 5 Gy. Either 30 min or 6 h after irradiation, the slides were washed with cold PBS, and cells were fixed with 4% formalin/PBS solution for 10 min at room temperature. Cells were then washed in PBS thrice, and mouse anti–human γ-H2AX (Abcam) was added at a dilution of 1:200 in antibody buffer and incubated overnight at 4°C. Cells were washed twice in PBS and incubated with a rhodamine red–labeled goat anti-mouse IgG secondary antibody (Molecular Probes) at a dilution of 1:500 in antibody buffer at room temperature for 45 min in the dark. The slides then were washed twice in PBS, and coverslips were mounted with glycerol/PBS (3:1) solution. Slides were examined on an Olympus fluorescent microscope and color print pictures were taken. Three random regions of 50 cells each were examined under microscope with ×100 magnification. Nuclei containing ≥10 foci (red color) were counted as positive for γ-H2AX foci formation. Percentage of positive cells were calculated and plotted.

***Western immunoblots.*** Cells were incubated with ABT-888 (5 μmol/L) and immediately irradiated with either 0 or 5 Gy. Fifteen, 30, or 240 min later, the treated cells were washed with iced-cold PBS twice before the addition of lysis buffer (20 nmol/L Tris, 150 mmol/L NaCl, 1 mmol/L EDTA, 1% Triton X-100, 2.5 mmol/L sodium NaPP*i*, 1 mmol/L phenylmethylsulfonyl fluoride, and leupeptin). Protein concentration was quantified by the Bio-Rad method. Equal amounts of protein were loaded into each well and separated by 10% SDS-PAGE gel, followed by transfer onto nitrocellulose membranes. Membranes were blocked by use of 5% nonfat dry milk in PBS for 1 h at room temperature. The blots were then incubated with poly(ADP-ribose) (PAR) antibodies (1:1,000; BD Biosciences) overnight at 4°C. Goat anti-rabbit IgG secondary antibodies (1:1,000; Santa Cruz Biotechnology) were incubated for 1 h at room temperature. Immunoblots were developed using the enhanced chemiluminescence detection system (Amersham) according to the manufacturer's protocol and autoradiography.

**In vitro *clonogenic assay.*** H460 human lung carcinoma cells were trypsinized and counted. Cells were diluted serially to appropriate concentrations and plated into 60-mm tissue culture dishes in 3 mL medium in triplicate per data point. The final drug concentration was 5 μmol/L in all plates. ABT-888 was added 24 h after cells were plated. Cells were then immediately irradiated with 0 to 6 Gy as indicated. Cells were incubated for 6 h, medium was aspirated, and fresh medium (3 mL) was then added. After treatment, cells were returned to 37°C incubation and maintained for 8 days. Cells were then fixed for 15 min with 3:1 (methanol/acetic acid) and stained for 15 min with 0.5% crystal violet (Sigma) in methanol. After staining, colonies were counted by the naked eye with a cutoff of 50 viable cells. The dose enhancement ratio (DER) was calculated as follows: DER = (dose of irradiation required for SF of 0.25) / (dose of irradiation with ABT-888 treatment required for SF of 0.25), where SF is the surviving fraction.

***Measurement of apoptosis.*** Levels of apoptosis were measured using Annexin V-FITC Apoptosis Detection kit I (BD PharMingen) with flow cytometry. H460 cells were plated into 100-mm dishes. After 24 h of 37°C incubation, the cells were treated with ABT-888 (5 μmol/L) and immediately irradiated with 3 Gy for radiation groups. Cells were then incubated for 6 h, the medium was aspirated, and fresh medium (3 mL) was added. Twelve hours after cells were treated with drug, cells were trypsinized (keeping all floating cells) and counted for each sample. Cells were washed twice with cold PBS and then resuspended in 1× binding buffer. One hundred microliters of the solution ($5 \times 10^5$ cells) were then transferred to a 5 mL culture tube, and 3 μL of Annexin V-FITC and 3 μL of propidium iodide were added. After 15-min incubation at room temperature in the dark, 400 μL of 1× binding buffer was added to each tube analyzed by FACScan.

***Green fluorescent protein–tagged light-chain 3 plasmid transfection.*** H460 cells were grown on sterile histologic slides in 15 mL medium, and after 24 h the cells were transfected with green fluorescent protein (GFP)–tagged light-chain 3 (LC3) plasmid (a gift from Dr. Norboru Mizushima, Department of Bioregulation and Metabolism, Tokyo Metropolitan Institute of Medical Science, Tokyo, Japan) using a mixture of LipofectAMINE (Life Technologies) and GFP-LC3 plasmid in Opti-MEM medium (Life Technologies) at a ratio of 12 μL LipofectAMINE per milliliter of medium per 2 μL plasmid. After 5 h of incubation, cells were placed in regular complete medium and cultured for 1 day. ABT-888 (5 μmol/L) or vehicle control was then added. After cells were irradiated with 3 Gy as indicated, the medium was changed, and cells were further incubated for 24 h at 37°C. The slides were then washed with cold PBS, and cells were fixed in cold methanol for 5 min at room temperature. Cells were then washed in PBS twice, and coverslips were mounted with glycerol/PBS (3:1) solution. Slides were examined on an Olympus fluorescent microscope and color pictures were taken.

***Endothelial cell morphogenesis assay: tube formation.*** Human umbilical vein endothelial cells were treated with ABT-888 (5 μmol/L) and then immediately treated with 3 Gy irradiation. After 6 h, cells were trypsinized and counted. They were seeded at 48,000 cells per well on 24-well plates coated with 300 μL of Matrigel (BD Biosciences). These cells undergo differentiation into capillary-like tube structures and were periodically observed using a microscope. After 24 h, cells were stained with H&E and photographs were taken via a microscope. The average number of tubes for three separate microscopic fields (×100) was counted and representative photographs were taken.

***Tumor volume assessment.*** Human NCI-H460 cells were used as a xenograft model in female athymic nude mice (nu/nu, 5-6 weeks old; Harlan Sprague-Dawley, Inc.). A suspension of $2 \times 10^6$ cells in 50 μL volume was injected s.c. into the left posterior flank of mice using a 1-mL syringe with 27.5-gauge needle. Tumors were grown for 6 to 8 days until average tumor volume reached 0.28 cm$^3$. Treatment groups consisted of vehicle control [5% DMSO in 0.9% saline (pH 5-6)], ABT-888 alone (drug solution adjusted from pH 9 to pH 5-6 by adding HCl), vehicle plus radiation, and ABT-888 plus radiation. Each treatment group contained five mice. Vehicle control and ABT-888 at doses of 25 mg/kg were administered i.p. for 5 consecutive days. Mice in radiation groups were irradiated 1 h after ABT-888 treatment with

2 Gy daily over 5 consecutive days. Tumors on the flanks of the mice were irradiated using an X-ray irradiator (Therapax, Agfa NDT, Inc.). The nontumor parts of the mice were shielded by lead blocks. Tumors were measured twice or thrice weekly in three perpendicular dimensions using a Vernier caliper with tumor volume calculated using the modified ellipsoid formula (length × width × height) / 2. Growth delay was calculated for treatment groups relative to control tumors.

***Histologic sections, von Willebrand factor, Ki67, and terminal deoxyribonucleotide transferase–mediated nick-end labeling staining.*** Mice were implanted with H460 as described above in the tumor volume studies. After 6 to 8 days, mice in the drug treatment group were treated with 25 mg/kg ABT-888, i.p. daily for 5 days. Mice in the radiation treatment group were irradiated as described above. After 5 days of daily treatments, mice were euthanized and tumors were paraffin fixed. Slides from each treatment group were then stained for von Willebrand factor using anti–von Willebrand factor polyclonal antibody (Chemicon). Blood vessels were quantified by randomly selecting ×400 fields and counting the number of blood vessels per field. This was done in triplicate and the average of the three counts was calculated. Ki67 and terminal deoxyribonucleotide transferase–mediated nick-end labeling (TUNEL) staining were done in our pathology core laboratory. The number of positive cells were scored and graphed by averaging three repeated assessments.

***Statistical analysis.*** Analysis of study results focused on testing the differences of the mean tumor volume among treatment groups and different time points. Data analysis was completed using the restricted/residual maximum likelihood-based, mixed-effect model to adjust the intracorrelation effect for the mice that had multiple measurements. The model reported in the article was selected on the basis of the Schwarz's Bayesian criterion. All tests of significance were two-sided, and differences were considered statistically significant when $P$ is <0.05. SAS version 8.2 was used for all analyses.

## Results

***PARP-1 inhibition attenuates radiation-induced PAR formation and reduces clonogenic survival.*** ABT-888 is an oral PARP inhibitor currently in development by Abbott Laboratories, which has shown promise in combination with chemotherapy in preclinical studies. Therefore, we sought to investigate the effect of this drug in combination with ionizing radiation in lung cancer models. To determine whether ABT-888 inhibits the function of PARP-1 in irradiated cells, a Western immunoblot was done to determine levels of PAR in H460 lung cancer cells. Cells were irradiated with 0 or 5 Gy in the presence or absence of 5 μmol/L ABT-888 and were incubated for various times. As shown in Fig. 1A, PAR levels are dramatically decreased by ABT-888 in both irradiated and nonirradiated cells to essentially undetectable levels.

Clonogenic assays were done on H460 lung cancer cells to determine whether inhibition of PARP-1 function in irradiated cells affects cell survival. A radiosensitizing effect was observed in cells treated with ABT-888 compared with vehicle control. ABT-888 (5 nmol/L) showed a moderate effect (data not shown), whereas 5 μmol/L ABT-888 significantly reduced clonogenic survival, showing a 10-fold decrease in cell survival at 6 Gy irradiation (Fig. 1B). To determine the magnitude of the radiosensitizing effect, the DER was calculated. The DER of ABT-888 was 1.27 ($P$ = 0.024).

***PARP-1 inhibition inhibits DNA repair in H460 lung cancer cells.*** To determine the effects of PARP-1 inhibition on DNA repair, fluorescence imaging was used to examine the expression of histone γ-H2AX in treated H460 cells. γ-H2AX has been established as a marker of double-stranded DNA breaks (18). At 30 min or 6 h after 5 Gy irradiation, cells were fixed and incubated with antibody for γ-H2AX, followed by a secondary antibody labeled with rhodamine red. Fluorescence microscope images were obtained (Fig. 2A and B) and the percentage of cells containing γ-H2AX foci was quantified (Fig. 2C). γ-H2AX nuclear foci–positive cells were diminished in irradiated cells at the 6-h time point after irradiation. However, the addition of ABT-888 significantly increased the percentage of cells containing γ-H2AX foci at 6 h compared with irradiation alone ($P$ = 0.009), suggesting that ABT-888 successfully inhibits DNA repair by PARP-1 inhibition.

***Increased apoptosis and autophagy in treated H460 cells.*** To determine the levels of apoptosis in treated cells, Annexin V–FITC was used to probe H460 cells. Percentage apoptosis was then measured using flow cytometry. Twenty-four hours before staining, cells were treated with ABT-888 (5 μmol/L) and irradiated with 3 Gy for radiation alone or combined groups. ABT-888 alone showed no increase in apoptosis compared with control, and 3 Gy increased apoptosis 2-fold. However, cells treated with both ABT-888 and 3 Gy showed a 2.8-fold increase

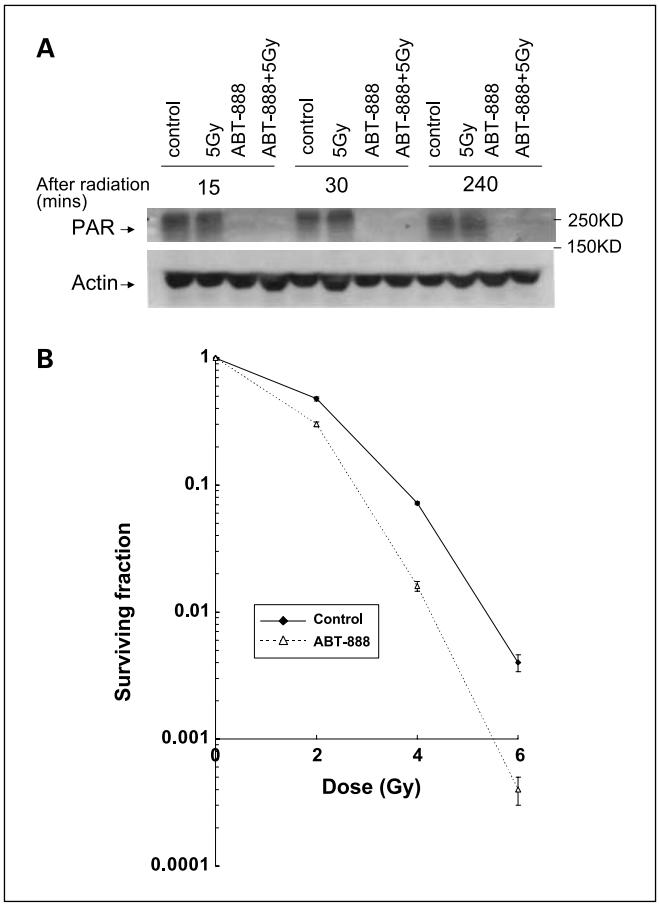


**Fig. 1.** PARP-1 inhibition attenuates radiation-induced PAR formation and reduces clonogenic survival. *A,* H460 lung carcinoma cells were incubated with ABT-888 5 μmol/L and immediately irradiated with 0 or 5 Gy. Total cell lysates were extracted 15, 30, or 240 min later. Equal amounts of protein per lane were probed with PAR antibodies. β-Actin was also probed to show equal loading. *B,* H460 cells were treated with either 5 μmol/L ABT-888 or a vehicle control, immediately followed by radiation doses of 0, 2, 4, or 6 Gy, and the drug was washed off after 6 h. After 8 d, colonies were stained and the scored colonies were graphed. Survival curves for H460 cells ± ABT-888 treatment. Points, mean; bars, SD ($P$ = 0.024).

in apoptosis (Fig. 3A; $P = 0.00002$ for ABT-888/radiation versus radiation alone).

Although apoptosis is an important means of cytotoxicity for cancer treatment, autophagy, or "self eating" has garnered attention as an alternative cell death pathway pertinent to cancer and radiation treatment. Autophagy is typically a controlled self-digestion process that allows for mobilization and recycling of metabolic materials. However, this self-digestion can ultimately proceed to cell death, and it is this capacity that is being sought for anticancer treatment. To determine whether PARP-1 inhibition combined with radiation induces autophagy in H460 cells, we transfected the cells with GFP-LC3 plasmid and detected the distribution of GFP. LC3 is a microtubule-associated protein that is a critical component of the autophagosome. The use of the GFP-tagged LC3 plasmid has become an effective marker for the autophagosome (19, 20). As shown in Fig. 3B, diffuse cytoplasmic localization of GFP-LC3 was observed in untreated H460 cells, whereas irradiated cells showed increased punctate fluorescence after 24 h. Increases in punctate fluorescence, indicating the presence of autophagic cells, was also observed in cells treated with ABT-888 alone and combination treatment. The increase in autophagic cells compared with control was 2.4-fold in the 3 Gy group, 3.7-fold after treatment with ABT-888 alone, and 7.3-fold after combination treatment (Fig. 3C; $P = 0.003$ for ABT-888/radiation versus radiation alone).

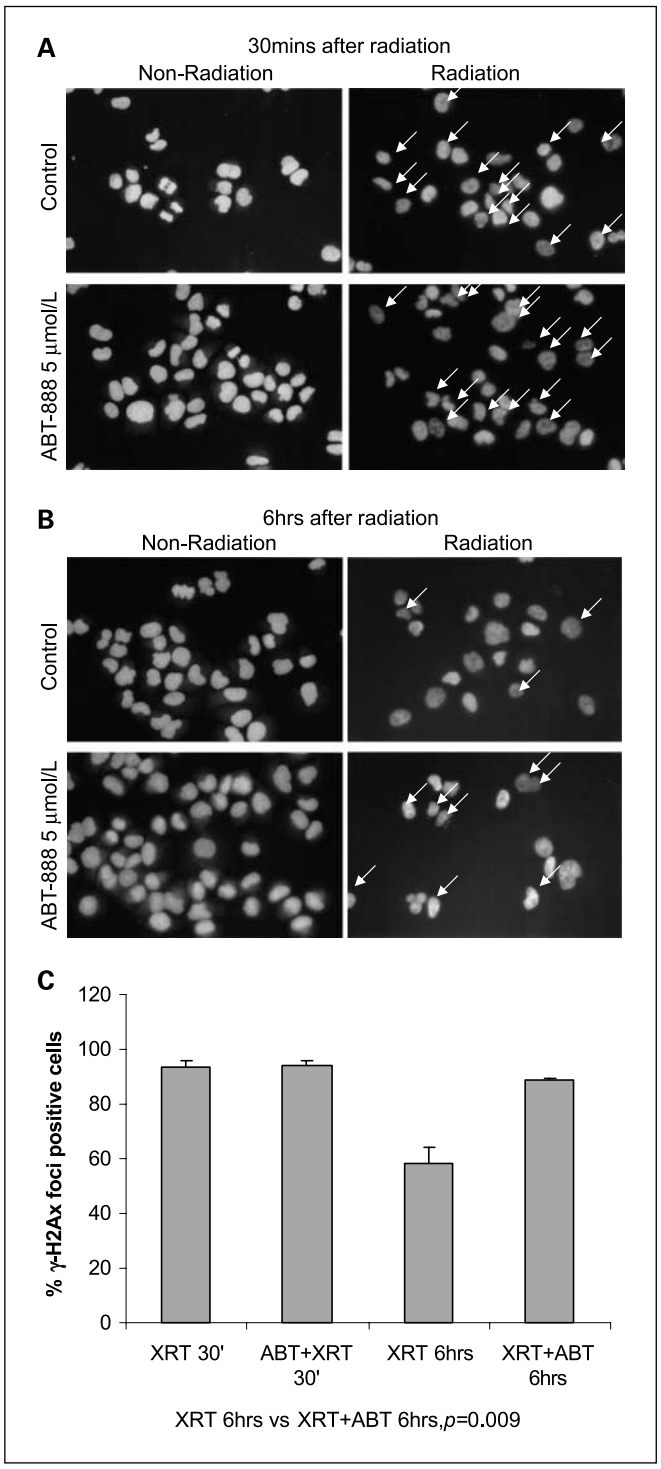


**Fig. 2.** PARP-1 inhibition inhibits DNA repair in H460 lung cancer cells. H460 cells were incubated with ABT-888 5 μmol/L and then immediately irradiated with either 0 or 5 Gy. Either 30 min (*A*) or 6 h (*B*) after irradiation, the slides were fixed and incubated with antibody for histone γ-H2AX, followed by a secondary antibody labeled with rhodamine red. Arrows, positive staining cells. Slides were examined on a fluorescent microscope and color print pictures were taken, and (*C*) the percentage of γ-H2AX foci containing cells was quantified ($P = 0.009$).

***Improved tumor growth delay with combined ABT-888 and radiotherapy at well-tolerated doses.*** To determine whether inhibition of PARP-1 enhances radiation-induced tumor growth delay, an H460 non–small cell lung cancer xenograft model was established and tumor volumes were measured by use of calipers, as previously described (21). Mice bearing H460 tumors were treated with ABT-888 25 mg/kg i.p. for 5 days and were then irradiated with 2 Gy fractions 1 h after drug administration, for a total dose of 10 Gy. For a 5-fold increase in tumor volume, ABT-888 and radiotherapy combination treatment induced a tumor growth delay of 13.5 days, compared with 1 day for ABT-888 alone and 7 days for radiation alone (Fig. 4A; $P = 0.045$ for ABT-888/radiation versus radiation alone).

The body weight changes were tracked in the mice to assess whether treatment with ABT-888, radiation, or combination yielded systemic toxicity. As shown in Fig. 4B, the control and drug-alone treatment groups showed minimal changes in weight (<3%). The radiation-alone group showed weight loss up to 15%; however, this toxic effect of the radiation dose was smaller in the combination treatment group, which only showed a 10% weight loss. Notably, the combination treatment group had less weight loss, despite having decreased tumor size, suggesting that the chosen dose of ABT-888 was well tolerated in the mice.

***ABT-888 with radiation reduces Ki67 proliferative marker and increases apoptotic index in H460 tumor models.*** To determine whether the tumor growth delay from the combined therapy results from decreased tumor proliferation and/or increased apoptosis, Ki67 and TUNEL staining was done using tissue sections from H460 tumors in all treatment groups. As shown in Fig. 5A and B, the Ki67 index was lowest in the combination treatment sections, a 2.6-fold decrease from the radiation alone group, and >7-fold reduction compared with the untreated controls ($P = 0.005$ for ABT-888/radiation versus radiation alone).

As shown in Fig. 5C and D, TUNEL staining indicated an approximate 65% increase in apoptosis when ABT-888 was added to radiotherapy ($P = 0.02$ for ABT-888/radiation versus

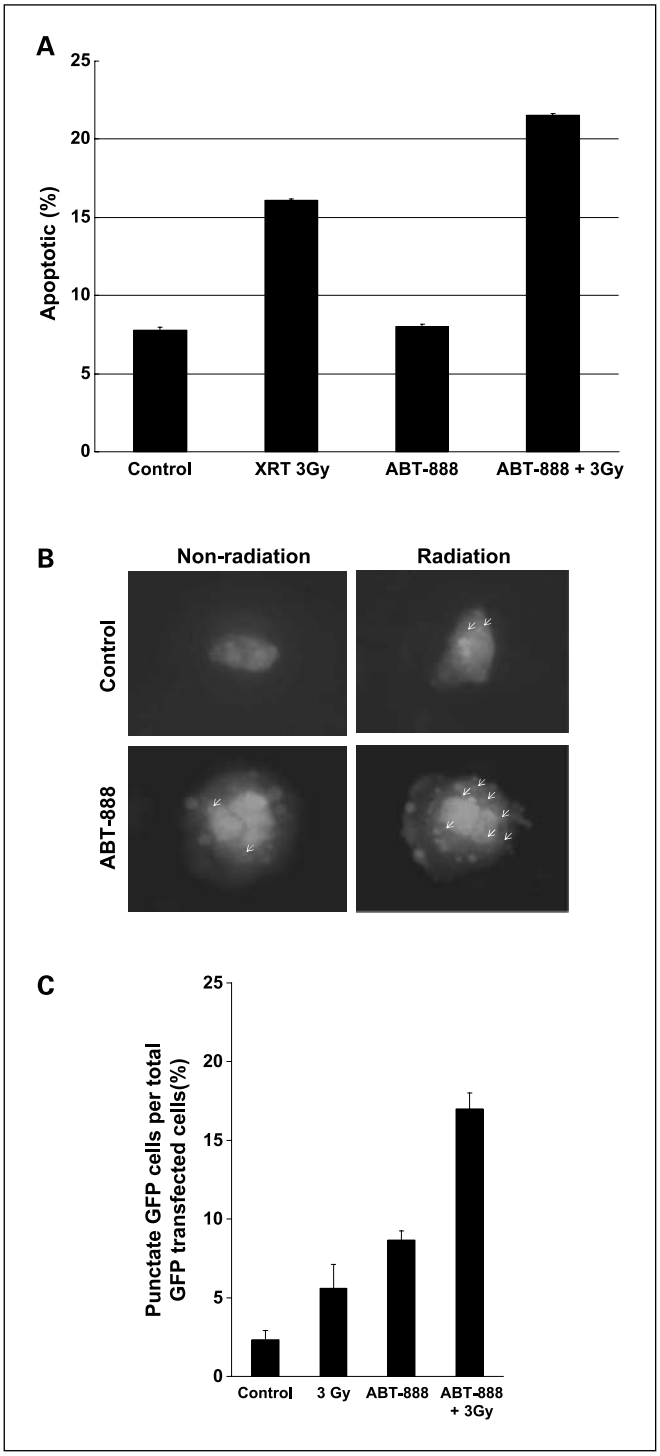


**Fig. 3.** Increased apoptosis and autophagy in treated H460 cells. *A,* H460 cells were treated with ABT-888 (5 μmol/L) and immediately irradiated with 3 Gy for radiation alone or combined groups. Cells were incubated for 6 h and then the medium was changed. Twenty-four hours after treatment, cells were incubated with Annexin V-FITC and propidium iodide, and analyzed by FACScan. The percentage of apoptotic cells for each group is shown. Data are shown as the mean of three experiments ± SD ($P = 0.00002$ for ABT-888/radiation versus radiation alone). *B,* GFP-LC3– transfected H460 cells were treated with ABT-888 (5 μmol/L) and immediately irradiated with 3 Gy for radiation alone or combined groups and then examined by fluorescence microscopy after 24 h. Punctate pattern of fluorescence seen in GFP-LC3– transfected H460 cells. Arrows, positive punctate staining examples. *C,* the percentage of cells with punctate GFP-LC3 fluorescence was calculated relative to all GFP-positive cells. Columns, mean; bars, SD ($P = 0.003$ for ABT-888/radiation versus radiation alone).

radiation alone). Additionally, the combination group shows a 7-fold increase in apoptosis compared with untreated controls.

***ABT-888 sensitizes vascular endothelial model to ionizing radiation and reduces vascular density in irradiated H460 tumors.*** To explore the effects of ABT-888 and radiation on blood vessel formation, we examined their effect on the angiogenic function of human umbilical vein endothelial cells *in vitro*. The formation of tubes by endothelial cells is a critical step in angiogenesis. The endothelial cell morphogenesis assay was done to examine the ability of treated human umbilical vein endothelial cells to produce capillary-like tubular structures. Representative photographs are shown in Fig. 6A, and the mean number of counted tubes in three separate (×100) fields is shown in Fig. 6B. No treatment control had 21 (SD 1.0) tubules per microscopic field, radiation alone had 16.3 (SD 1.2) tubules, ABT-888 alone had 15 (SD 1.0) tubules, and ABT-888/radiation combination had 5 (SD 1.0) tubules ($P = 0.006$ for ABT-888/radiation versus radiation alone).

To determine the effects of ABT-888 and radiation on tumor vasculature *in vivo*, mice were treated similarly to those in the tumor growth delay study, with daily 25 mg/kg ABT-888 administration followed by 2 Gy fractionated radiation treatments for 5 days. After 5 days, the tumors were resected and paraffin-fixed, and an antibody for von Willebrand factor was used to stain for blood vessels. A representative image is shown in Fig. 6C. The number of vessels per microscopic field was then determined for each treatment group. Control tumors had an average of 11 (SD 1.0) vessels per microscopic field, drug alone had 7.3 (SD 0.6) vessels, radiation alone had 4 (SD = 1.0), and combination had 1.6 (SD 0.6; $P = 0.02$ for ABT-888/radiation versus radiation alone; Fig. 6D).

## Discussion

In the present study, we found that the PARP inhibitor, ABT-888, sensitizes H460 lung cancer cells to radiation, and both increased apoptosis and autophagy were shown to contribute to the increase in clonogenic cell death. Using histone γ-H2AX as a marker for DNA strand breaks, we showed that ABT-888 inhibited DNA repair in irradiated H460 cells. Combination treatment with ABT-888 and radiation also enhanced tumor growth delay in an H460 xenograft model by inhibiting tumor proliferation, promoting apoptosis, and reducing tumor vascular density.

Due to therapeutic limitations imposed by the development of chemoresistance and radioresistance in tumors, DNA repair proteins are becoming an important target for enhancing cancer therapy (22). In particular, PARP-1 is becoming a leading target due to its central involvement in DNA repair signaling (9, 23, 24). PARP-2, a closely related protein, has also been implicated in this pathway (25). PARP-1 and PARP-2 have been proposed to act as both DNA damage sensors and signal transducers to downstream effectors of cell cycle arrest and DNA repair (26). After binding damaged DNA with its zinc finger binding motif, activated PARP-1 uses $NAD^+$ as a substrate to catalyze its automodification, as well as modification of other nuclear proteins by adding ADP-ribose polymers (27). PARP-2 has also been shown to undergo the same automodification and can homodimerize or heterodimerize with PARP-1 (25, 28). PAR then binds specific proteins involved in DNA repair, cell cycle progression, and cell death,

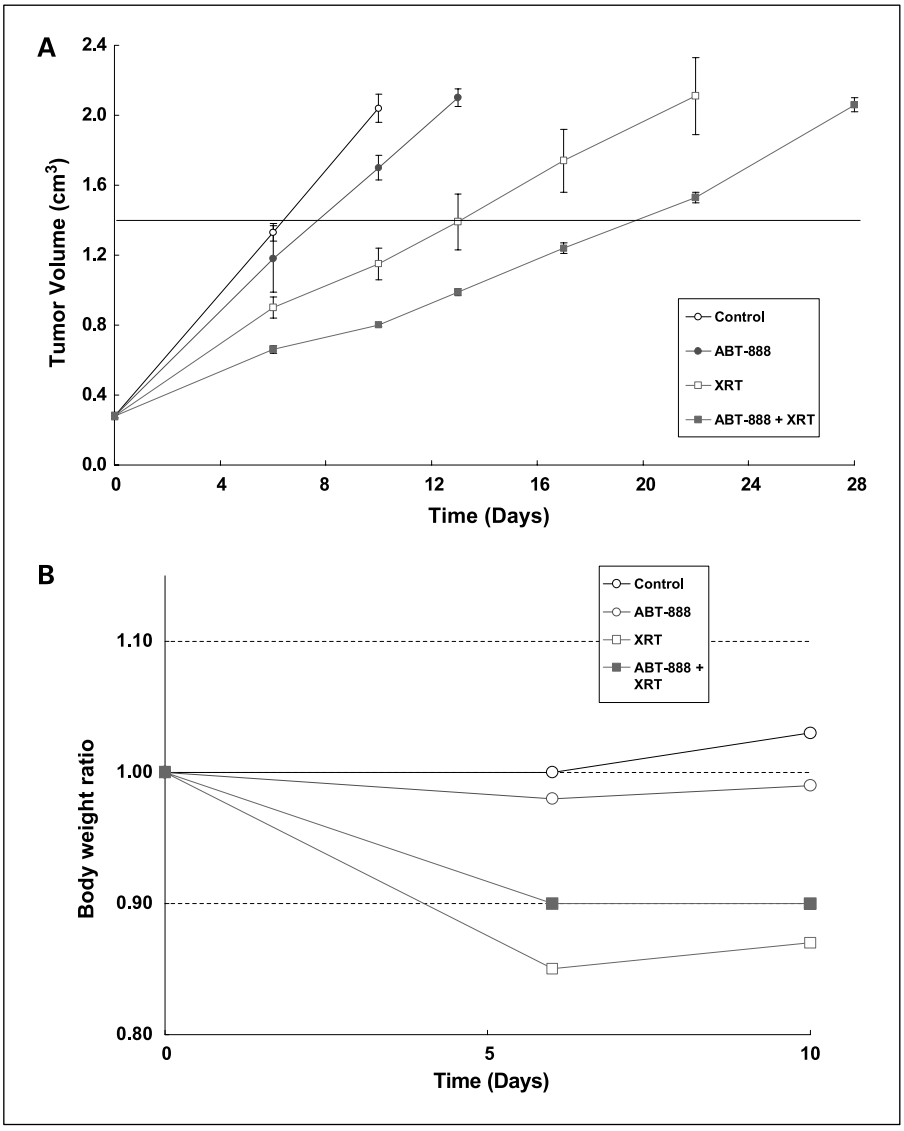


**Fig. 4.** Improved tumor growth delay with combined ABT-888 and radiotherapy at well-tolerated doses. H460 tumors were implanted into the posterior flank of nude mice. Mice were treated with vehicle control or 25 mg/kg (i.p.) ABT-888 for 5 consecutive days, and mice in radiation groups were irradiated 1 h after drug treatment with 2 Gy daily for 5 d. *A,* tumor volume was measured with calipers at the indicated time points and is shown for each treatment group ($P = 0.045$ for ABT-888/radiation versus radiation alone at day 22). *B,* the average weight for each treatment group was also measured.

and modifies their functions (27). For example, X-ray repair cross-complementing protein 1 (XRCC1) is a protein that is recruited to DNA damage sites and acts as a scaffold to coordinate base excision repair. XRCC1 has been shown to preferentially interact with (ADP-ribosyl)ated PARP-1 and PARP-2 (28, 29), and XRCC1 is recruited to sites of PAR formation in living cells (30). DNA ligase III, another important enzyme in base excision repair, has been isolated in a complex with PARP-1 and XRCC1 in DNA-damaged cells, and this complex is not found when PARP-1 is inhibited (31).

PARP signaling has also been implicated in the activation of other downstream cellular effectors after DNA damage. For example, p53 binds activated PARP-1 with high affinity (32), and PAR synthesis is important for the activation of p53 after irradiation and for p53-dependent cell cycle arrest (33). The functions of p53 are also inhibited when PARP is inhibited or knocked out (34, 35). Many DNA damage effectors, including XRCC1, DNA ligase III, p53, p21, DNA-PK, and nuclear factor-κB, have been shown to contain analogous PAR-binding motifs that overlap with functional domains (36).

The present study found that the potent PARP-1, PARP-2 inhibitor, ABT-888, effectively attenuated PAR formation at 5 μmol/L (Fig. 1A). This suggests that after ABT-888 treatment, the inhibition of PARP-1 automodification and the absence of PAR would prevent the recruitment of DNA repair machinery. To test this hypothesis, we compared irradiated ABT-888–treated H460 cells with irradiated controls and probed the cells with an antibody for histone γ-H2AX, a marker of DNA damage (18). As expected, we found that both treated and untreated cells contained increased levels of γ-H2AX foci 30 min after irradiation, indicating radiation-induced DNA damage. However, 6 h after irradiation, the control cells showed minimal expression of γ-H2AX foci, whereas the ABT-888–treated cells showed no decrease in γ-H2AX, indicating that DNA repair was inhibited (Fig. 2A-C). Clonogenic assays confirmed that ABT-888 potentiates the cytotoxic effects of radiation in H460 cells (Fig. 1B).

The induction of autophagy by radiation has been previously reported in cancer cells (37), but to our knowledge has not been reported in irradiated lung cancer cells. Additionally, the

present study shows that PARP-1 inhibition can induce autophagy and that combination of PARP-1 inhibition with radiation results in significant induction of autophagy compared with radiation alone ($P = 0.003$; Fig. 3B and C). We also found that although ABT-888 alone did not induce apoptosis above control levels, the drug enhanced radiation-induced apoptosis (Fig. 3A).

To the authors' knowledge, the present study is the first to examine the combination of PARP inhibition and radiotherapy in a lung cancer model *in vivo* and the first to explore the combination of ABT-888 and radiation. Consistent with our *in vitro* results, ABT-888 substantially potentiated the tumor growth delay induced by radiation while having minimal effect as monotherapy. For a 5-fold increase in tumor volume, tumor growth delay was 1 day for ABT-888 alone, 7 days for radiation alone, and 13.5 days for combination treatment (Fig. 4A). This is consistent with a previous study that found that PARP-1 inhibitor AG14361 improves radiation-induced tumor growth delay in colon adenocarcinoma xenografts (11), although few studies have examined the combination PARP-1 inhibitors and

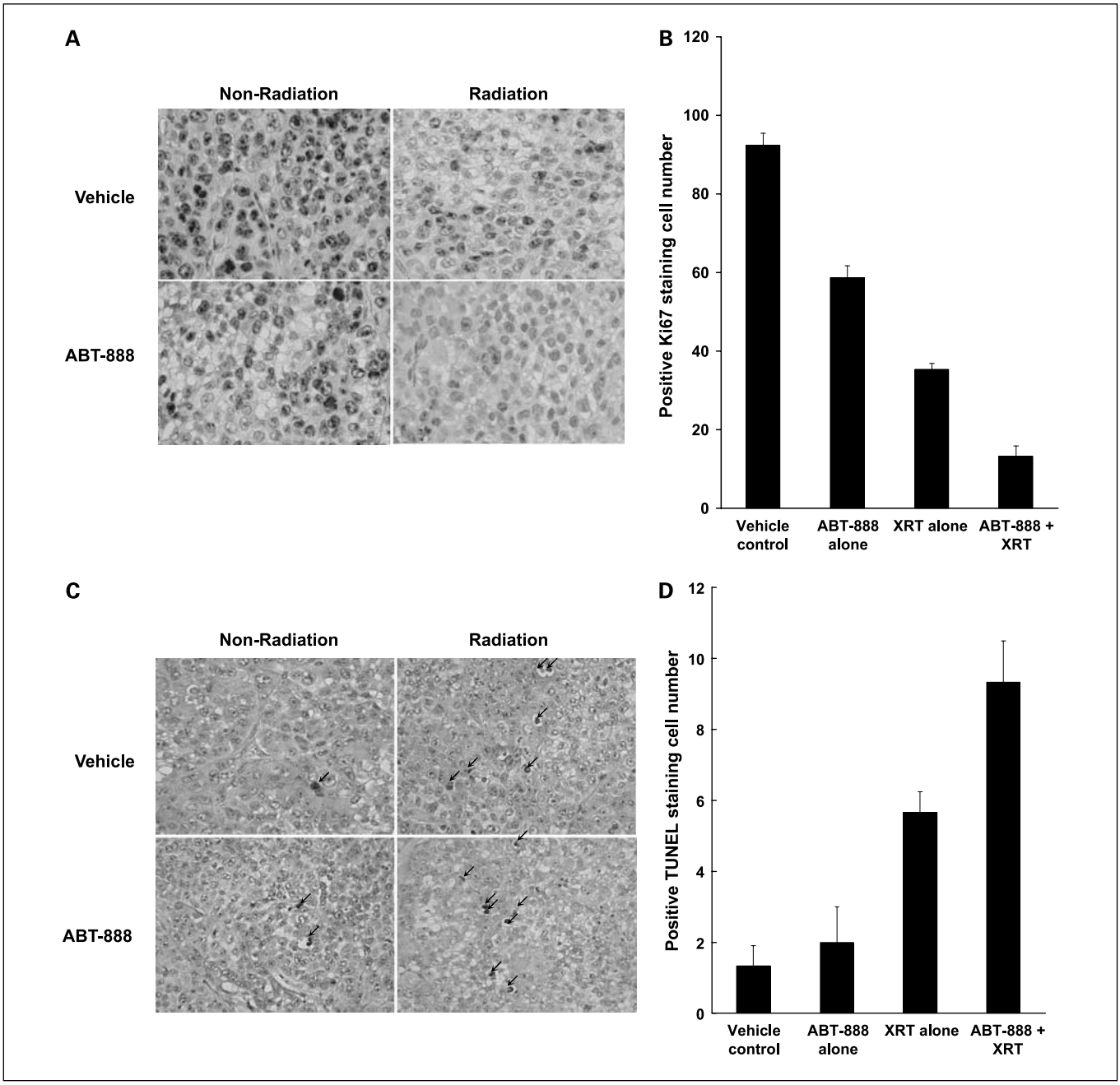


**Fig. 5.** ABT-888 with radiation reduces Ki67 proliferative marker and increases apoptotic index in H460 tumor models. Histologic sections were obtained from the tumors of the mice in each treatment group. *A,* standard Ki67 staining was done and representative images are shown. *B,* average proliferative index of each treatment group was determined by counting positive cells per microscopic field. This was repeated thrice. Columns, mean; bars, SD ($P = 0.005$ for ABT-888/radiation versus radiation alone). *C,* TUNEL staining was also done on tumor sections and representative images are shown. Arrows, TUNEL-positive cells. *D,* apoptotic index was similarly calculated by counting positive cells per microscopic field. Column, mean; bars, SD ($P = 0.02$ for ABT-888/radiation versus radiation alone).

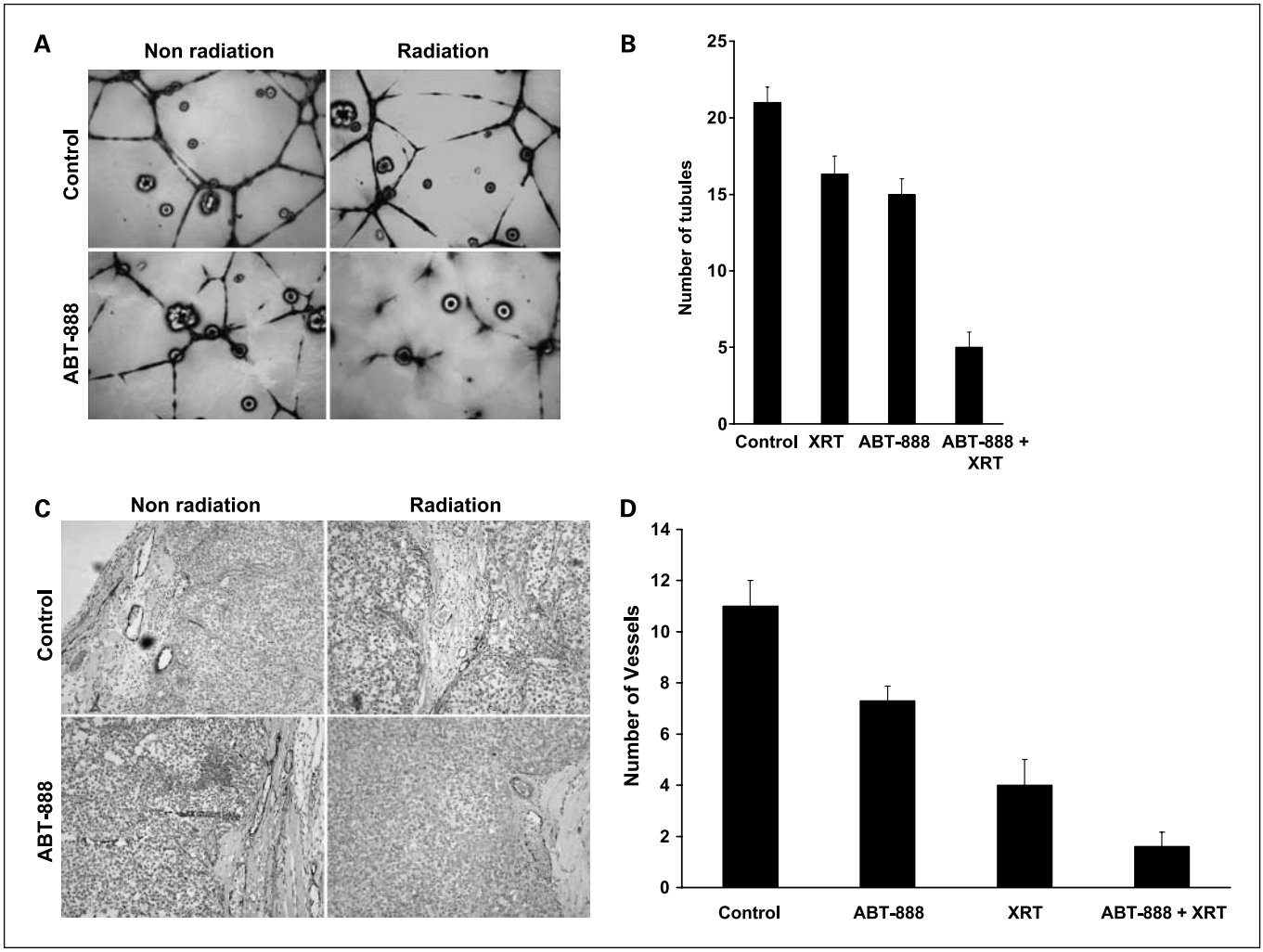


**Fig. 6.** ABT-888 sensitizes vascular endothelial model to ionizing radiation and reduces vascular density in irradiated H460 tumors. *A,* human umbilical vein endothelial cells were treated with 5 μmol/L ABT-888 and then immediately irradiated with either 0 or 3 Gy. Six hours later, cells were trypsinized and replated on 24-well plates coated with Matrigel. After 24 h, cells were fixed and stained with H&E. The slides were examined by microscopy (×100). Stained tubules were then counted in three separate, randomly selected fields, and representative fields are shown in (*A*). *B,* columns, mean number of tubules counted per microscopic field; bars, SD [$P = 0.006$ for ABT-888/radiation versus radiation (*XRT*) alone]. *C,* mice were treated similarly to those in the tumor growth delay study, with daily 25 mg/kg ABT-888 administration followed by 2 Gy radiation fractions for 5 d. Histologic sections were obtained from the tumors of the mice in each treatment group and stained for blood vessels using an antibody for von Willebrand factor. Magnification of representative sections from each treatment group, ×400. *D,* average blood vessel density of each treatment group was determined by counting the number of blood vessels per microscopic field. This was repeated thrice. Columns, average; bars, SD ($P = 0.02$ for ABT-888/radiation versus radiation alone).

radiotherapy *in vivo*. We also explored the mechanism of tumor growth delay. There was a notable decrease in Ki67 staining of mice that received combination treatment, compared with control or either treatment alone, with the combination treatment group showing a 7-fold decrease in Ki67 staining compared with untreated control (Fig. 5A and B). Similarly, apoptosis was increased in the combination treatment group compared with controls (Fig. 5C and D). These data suggest that the mechanism of tumor growth delay included both decreased proliferation and increased apoptosis of tumor cells.

Another important consideration when evaluating novel antineoplastic therapeutics is their effect on angiogenesis. We show that ABT-888 in combination with radiation decreases the ability of endothelial cells to form capillary tubule-like structures compared with drug or radiation alone (Fig. 6A and B). To further explore the effect of treatment on tumor vasculature *in vivo*, we used von Willebrand factor staining of tumor histologic sections and showed that tumor vascular density is decreased by combination therapy (Fig. 6C and D). Radiotherapy is known to provide tumor antiangiogenic effects in addition to its direct cytotoxic effects on tumor cells (38, 39). Although little work has focused on the effects of PARP-1 inhibitors on tumor vasculature, one study found that PARP-1 inhibitor AG14361 increased transient perfusion within tumors (11). In that study, they examined the effects of PARP-1 inhibition on tumor blood flow within a 1-h period and concluded that AG14361 transiently increases tumor blood. In our study, we examined the effects of PARP-1 inhibition on tumor vasculature after 5 days. The decreased number of tumor vessels after combination treatment compared with radiation alone shows that ABT-888 enhances the antiangiogenic effects of radiotherapy. One recent study found that insulin-like growth factor-1 induces vascular endothelial growth factor expression through inhibition of PARP-1, and that PARP-1

inhibition enhances vascular endothelial growth factor expression (40). However, these effects were modest and it is likely that any vascular endothelial growth factor expression induced by PARP-1 inhibition does not compensate for radiation enhancement on tumor vasculature *in vivo*.

Properly using the PARP signaling pathway will be important as potent PARP inhibitors are developed for clinical use. Although the PARP family has been well studied, there remains some uncertainty regarding the role of PARP proteins in cell survival and cell death. It has been proposed that after mild DNA damage, PARP facilitates DNA repair and enhances cell survival, but more severe DNA damage results in insufficient DNA repair and activation of apoptosis. The most severe DNA damage results in overactivation of PARP and depletion of cellular $NAD^+$ and ATP, blocking apoptosis and leading to necrosis (24, 41). As a result, the role of PARP in DNA damage signaling has been termed a double-edged sword. Additionally, it has been shown that PARP-2 can partially compensate for the loss of PARP-1 activity, and that loss of PARP-1 and PARP-2 is incompatible with development (42). Although PARP-2 is primarily located in the perinuclear region in PARP-1+/+ MEF cells, PARP-2 is localized to the nucleus in MEF PARP-1-/- knockout cells. Notably, PARP-2 was found to localize to the nucleus 6 h after low-dose irradiation in the PARP-1+/+ cells (12). This suggests that inhibiting both PARP-1 and PARP-2 may provide the best potentiation of the cytotoxic effects of radiation. Because ABT-888 is a small molecule, orally administered inhibitor of both PARP-1 and PARP-2, this drug shows promise as a clinical therapeutic. *In vitro*, the $K_i$ for PARP-1 and PARP-2 are 3.6 and 2.9 nmol/L, respectively. However, *in vivo* studies have shown that optimal efficacy occurs at ~25 mg/kg/d, which is the dose used for our studies. The drug has good bioavailability, particularly in mice (92%), whereas predicted oral bioavailability for humans is ~70%. The Cancer Therapy Evaluation Program has solicited both preclinical and phase I combination-agent studies. Currently, a phase 0 trial is under way.

It has been shown that expression of the genes encoding PARP-1 and PARP-2 is increased during development and increased in the highly proliferative cell compartments of adult mice. Murine tumors also displayed high levels of PARP-1 and PARP-2 expression compared with normal tissue (28). Although high levels of PARP-1 and PARP-2 have also been observed in nonproliferating tissue, this suggests that use of PARP inhibitors may provide some degree of molecular targeting in addition to the spatial targeting provided by radiotherapy.

In the present study, we used PARP-1 inhibitor ABT-888 in combination with radiation in non–small cell lung cancer models. ABT-888 is a novel potent small-molecule PARP-1 inhibitor that is currently in a dose escalation phase 0 clinical trial for refractory solid tumors and lymphoid malignancies. However, the use of this agent with radiation has not been previously explored. Our data provide evidence to support the efficacy and feasibility of combining ABT-888 with radiotherapy, and also provide further evidence supporting the use of PARP-1 inhibitors to potentiate the effects of radiation. Future clinical studies are needed to determine the efficacy of ABT-888 in combination with radiotherapy in lung cancer patients.



## References


1. Schreiber V, Hunting D, Trucco C, et al. A dominant-negative mutant of human poly(ADP-ribose) polymerase affects cell recovery, apoptosis, and sister chromatid exchange following DNA damage. Proc Natl Acad Sci U S A 1995;92:4753–7.
2. de Murcia JM, Niedergang C, Trucco C, et al. Requirement of poly(ADP-ribose) polymerase in recovery from DNA damage in mice and in cells. Proc Natl Acad Sci U S A 1997;94:7303–7.
3. Dantzer F, Schreiber V, Niedergang C, et al. Involvement of poly(ADP-ribose) polymerase in base excision repair. Biochimie 1999;81:69–75.
4. Dantzer F, de La Rubia G, Menissier-De Murcia J, Hostomsky Z, de Murcia G, Schreiber V. Base excision repair is impaired in mammalian cells lacking Poly (ADP-ribose) polymerase-1. Biochemistry 2000;39: 7559–69.
5. Lindahl T, Wood RD. Quality control by DNA repair. Science 1999;286:1897–905.
6. Schreiber V, Dantzer F, Ame JC, de Murcia G. Poly (ADP-ribose): novel functions for an old molecule. Nat Rev Mol Cell Biol 2006;7:517–28.
7. Szumiel I. Monitoring and signaling of radiation-induced damage in mammalian cells. Radiat Res 1998;150:S92–101.
8. Satoh MS, Poirier GG, Lindahl T. NAD(+)-dependent repair of damaged DNA by human cell extracts. J Biol Chem 1993;268:5480–7.
9. Tentori L, Graziani G. Chemopotentiation by PARP inhibitors in cancer therapy. Pharmacol Res 2005;52: 25–33.
10. Veuger SJ, Curtin NJ, Richardson CJ, Smith GC, Durkacz BW. Radiosensitization and DNA repair inhibition by the combined use of novel inhibitors of DNA-dependent protein kinase and poly(ADP-ribose) polymerase-1. Cancer Res 2003;63:6008–15.
11. Calabrese CR, Almassy R, Barton S, et al. Anticancer chemosensitization and radiosensitization by the novel poly(ADP-ribose) polymerase-1 inhibitor AG14361. J Natl Cancer Inst 2004;96:56–67.
12. Chalmers A, Johnston P, Woodcock M, Joiner M, Marples B. PARP-1, PARP-2, and the cellular response to low doses of ionizing radiation. Int J Radiat Oncol Biol Phys 2004;58:410–9.
13. Ries L, Eisner MP, Kosary CL, et al., editors. SEER cancer statistics review, 1975-2002. Bethesda (MD): National Cancer Institute; 2005.
14. Zeng-Rong N, Paterson J, Alpert L, Tsao MS, Viallet J, Alaoui-Jamali MA. Elevated DNA repair capacity is associated with intrinsic resistance of lung cancer to chemotherapy. Cancer Res 1995;55:4760–4.
15. Bosken CH, Wei Q, Amos CI, Spitz MR. An analysis of DNA repair as a determinant of survival in patients with non-small-cell lung cancer. J Natl Cancer Inst 2002;94:1091–9.
16. Duchesne GM. Fundamental bases of combined therapy in lung cancer: cell resistance to chemotherapy and radiotherapy. Lung Cancer 1994;10 Suppl 1: S67–72.
17. Guo WF, Lin RX, Huang J, et al. Identification of differentially expressed genes contributing to radioresistance in lung cancer cells using microarray analysis. Radiat Res 2005;164:27–35.
18. Rogakou EP, Boon C, Redon C, Bonner WM. Megabase chromatin domains involved in DNA double-strand breaks *in vivo*. J Cell Biol 1999;146:905–16.
19. Demarchi F, Schneider C. The calpain system as a modulator of stress/damage response. Cell Cycle 2007;6:136–8.
20. Martinet W, Verheye S, De Meyer GR. Everolimus-induced mTOR inhibition selectively depletes macrophages in atherosclerotic plaques by autophagy. Autophagy 2007;3:241–4.
21. Edwards E, Geng L, Tan J, Onishko H, Donnelly E, Hallahan DE. Phosphatidylinositol 3-kinase/Akt signaling in the response of vascular endothelium to ionizing radiation. Cancer Res 2002;62:4671–7.
22. Madhusudan S, Middleton MR. The emerging role of DNA repair proteins as predictive, prognostic and therapeutic targets in cancer. Cancer Treat Rev 2005; 31:603–17.
23. Soldatenkov VA, Smulson M. Poly(ADP-ribose) polymerase in DNA damage-response pathway: implications for radiation oncology. Int J Cancer 2000;90:59–67.
24. Tentori L, Portarena I, Graziani G. Potential clinical applications of poly(ADP-ribose) polymerase (PARP) inhibitors. Pharmacol Res 2002;45:73–85.
25. Ame JC, Rolli V, Schreiber V, et al. PARP-2, A novel mammalian DNA damage-dependent poly(ADP-ribose) polymerase. J Biol Chem 1999;274:17860–8.
26. Althaus FR, Kleczkowska HE, Malanga M, et al. Poly ADP-ribosylation: a DNA break signal mechanism. Mol Cell Biochem 1999;193:5–11.
27. Malanga M, Althaus FR. The role of poly(ADP-ribose) in the DNA damage signaling network. Biochem Cell Biol 2005;83:354–64.
28. Schreiber V, Ame JC, Dolle P, et al. Poly(ADP-ribose) polymerase-2 (PARP-2) is required for efficient base excision DNA repair in association with PARP-1 and XRCC1. J Biol Chem 2002;277:23028–36.
29. Masson M, Niedergang C, Schreiber V, Muller S, Menissier-de Murcia J, de Murcia G. XRCC1 is specifically associated with poly(ADP-ribose) polymerase and negatively regulates its activity following DNA damage. Mol Cell Biol 1998;18:3563–71.
30. Okano S, Lan L, Caldecott KW, Mori T, Yasui A. Spatial and temporal cellular responses to single-strand breaks in human cells. Mol Cell Biol 2003;23: 3974–81.
31. Leppard JB, Dong Z, Mackey ZB, Tomkinson AE. Physical and functional interaction between DNA

ligase IIIα and poly(ADP-ribose) polymerase 1 in DNA single-strand break repair. Mol Cell Biol 2003;23:5919–27.

**32.** Malanga M, Pleschke JM, Kleczkowska HE, Althaus FR. Poly(ADP-ribose) binds to specific domains of p53 and alters its DNA binding functions. J Biol Chem 1998;273:11839–43.

**33.** Wieler S, Gagne JP, Vaziri H, Poirier GG, Benchimol S. Poly(ADP-ribose) polymerase-1 is a positive regulator of the p53-mediated $G_1$ arrest response following ionizing radiation. J Biol Chem 2003;278:18914–21.

**34.** Wang X, Ohnishi K, Takahashi A, Ohnishi T. Poly(ADP-ribosyl)ation is required for p53-dependent signal transduction induced by radiation. Oncogene 1998;17:2819–25.

**35.** Valenzuela MT, Guerrero R, Nunez MI, et al. PARP-1 modifies the effectiveness of p53-mediated DNA damage response. Oncogene 2002;21:1108–16.

**36.** Pleschke JM, Kleczkowska HE, Strohm M, Althaus FR. Poly(ADP-ribose) binds to specific domains in DNA damage checkpoint proteins. J Biol Chem 2000;275:40974–80.

**37.** Paglin S, Hollister T, Delohery T, et al. A novel response of cancer cells to radiation involves autophagy and formation of acidic vesicles. Cancer Res 2001;61:439–44.

**38.** Garcia-Barros M, Paris F, Cordon-Cardo C, et al. Tumor response to radiotherapy regulated by endothelial cell apoptosis. Science 2003;300:1155–9.

**39.** Wachsberger P, Burd R, Dicker AP. Tumor response to ionizing radiation combined with antiangiogenesis or vascular targeting agents: exploring mechanisms of interaction. Clin Cancer Res 2003;9:1957–71.

**40.** Beckert S, Farrahi F, Perveen Ghani Q, et al. IGF-I-induced VEGF expression in HUVEC involves phosphorylation and inhibition of poly(ADP-ribose) polymerase. Biochem Biophys Res Commun 2006;341:67–72.

**41.** Virag L, Szabo C. The therapeutic potential of poly(ADP-ribose) polymerase inhibitors. Pharmacol Rev 2002;54:375–429.

**42.** Menissier de Murcia J, Ricoul M, Tartier L, et al. Functional interaction between PARP-1 and PARP-2 in chromosome stability and embryonic development in mouse. EMBO J 2003;22:2255–63.